Magnetic Induction Sensor for the Respiration Monitoring

J. Ojarand, S. Pille
ELIKO Competence Centre
Tallinn, Estonia
jaan.ojarand@eliko.ee

M. Min, R. Land, J. Oleitšuk
Tallinn University of Technology
Tallinn, Estonia
min@elin.ttu.ee

***Abstract*—Bio-sensing technologies are of increasing importance in healthcare, sport and security sectors. The respiration and pulse rates are the important vital signs of persons. Telemonitoring systems with contactless sensors allow collection of data in the situations where the ease of positioning of sensors and the mobility of persons are required. The telemonitoring system presented in this paper is based on the magnetic eddy current induction sensor. The influence of properties and placement of the sensor on the sensitivity of measurements is characterized. An imitator of the impedance of lungs was designed for the steady comparison of measurement results. Measurements in healthy volunteers demonstrated the ability of the system to monitor respiration.**

Keywords—magnetic induction sensor; respiratory monitoring; telemonitoring.

I. INTRODUCTION

The respiration and pulse rates are the important vital signs of persons that are widely used in healthcare, sport and security sectors. In the last two cases, the wireless telemonitoring is essential. However, sometimes the limitation of a patient's mobility should also be avoided in the healthcare applications. Furthermore, use of wireless connection meets better the safety requirements and improves the signal to noise ratio (SNR) of measurements since the ground loop of disturbance currents is broken.

The magnetic induction monitoring is a non-contact monitoring technique, which meets most of the requirements described above. Common techniques for magnetic eddy current induction measurements are based on a multiple coil method [1], [2]. Our main target was testing of magnetic induction monitoring technique for the life vest application. Since multiple coils have to be precisely calibrated in a geometric alignment, this setup does not suit well to our case. Therefore, a method based on a single coil is used. This method was introduced in 1967 and has occasionally been investigated by four research groups [3].

Recently a pulse and respiratory monitoring system with multiple flexible coils that were sewn into the shirt was presented in [3]. In this study, the coils were used as a part of a Colpitts oscillator. The frequency change due to a variation in coil impedance was measured by a frequency counter realized by using the counter input of a microcontroller.

In the present study, a high-resolution inductance-to-digital converter LDC1000 (Texas Instruments, Dallas, TX, USA) is employed that simultaneously measures the impedance and resonant frequency of an LC resonator. Measurement of the impedance allows better estimation of eddy currents than the use of frequency changes as explained in the next sections.

The sensitivity of the measurement system was tested with a set of planar coils. The flexible ferrite sheets were used for rejecting of the extraneous disturbances and inductive couplings. Also, their influence on the sensitivity of measurements was tested.

Since many unrepeatable factors influence the live respiration measurements, an imitator of the impedance of lungs was designed for the steady comparison of results. The measurements results of the healthy volunteer are also provided for validation.

II. SENSING PRINCIPLE

A. General Aspects

The magnetic field sent out by the sensor coil induces thoracic eddy currents, which reinduce a secondary magnetic field changing the reflected impedance of the coil (Fig. 1.).

A sensor coil driven by an alternating current excites an alternating magnetic field, B_1, which induces eddy currents within the thorax. These eddy currents excite another alternating magnetic field, B_2, in turn, whose size and orientation depends on the distribution of thoracic impedance.

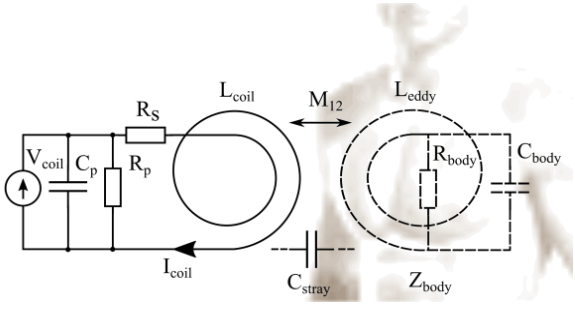

Fig. 1. A simplified model of the sensing principle.

B. A Single Coil Sensor Solution

Considering that the reinduced field affects the primary one, a single coil can monitor the thorax impedance using the so-called reflected impedance of the excitation coil $Z_{co,r}$. Employing a traditional transformer model with mutual inductance M_{12} the complex reflected coil impedance can be expressed by [3]:

$$\dot{Z}_{co,r} = R_s + j\omega L_{co} - \frac{\omega^3 C_{body} M_{12}^2}{j\omega C_{body}(R_{body} + j\omega L_{eddy}) + 1} \quad (1)$$

Note that the stray capacitance C_{stray} is omitted in this equation, assuming that the distance between the coil surface and the thoracic wall is constant. If this distance is changing, it reflects in $Z_{co,r}$ due to the changes of stray capacitance and magnetic coupling factor k.

Other important factors that are affecting the reflected impedance of the coil and enabling the vital sign monitoring are the changes of thoracic impedance. The physiological activity (i.e., respiration and pulse) modulates this impedance in several ways. The volumes of organs, tissue or blood, are varied which causes the changes in conductivity. The displacement of inner and outer boundaries of organs changes the direction and length of current paths. A change in the form of the excitation coil or the eddy current paths (by organ displacement) would change the magnetic coupling factor k as well the inductances L_{co} and L_{eddy}.

C. Single Coil Sensor using the LDC1000 Converter

In the present study, a high-resolution inductance-to-digital converter LDC1000 is used that measures the impedance of an LC resonator. It accomplishes this task by regulating the oscillation amplitude in a closed loop configuration to a constant level while monitoring the energy dissipated by the resonator. By monitoring the amount of power injected into the resonator, the LDC1000 can determine the value of the equivalent parallel resonance impedance R_p as

$$R_p = \frac{L_{co} + L_d}{(R_s + R_d)C_p} \quad (2)$$

R_s represents the coil's series resistance and R_d, L_d the reflected resistance of R_{body} and L_{eddy} respectively. C_p is a total parallel capacitance of the LC resonator including the capacitances of the fixed capacitor C, reflected capacitance of C_{body}, coil's capacitance C_L and stray capacitance C_{stray}

If the value of C is kept significantly higher than the sum of other components and L_{co} >> L_d then the value of the equivalent parallel resonance impedance R_p follows mainly the changes of the reflected resistance of R_{body}.

In addition, the LDC1000 can also measure the oscillation frequency of the LC circuit; this frequency is used to determine the inductance of the LC circuit.

III. Measurement System Setup

A. System Overview

The measurement system contains the master controller module (MCM) and slave sensor modules communicating via half-duplex RS-485 interface, Fig.2. The MCM is placed in a small plastic box that also contains a 3.7 V lithium-polymer battery and Wi-Fi transmitter, Fig. 3. There is a total of four wires between the master and slave modules. The same wires are also used for charging the battery. Up to 16 sensor modules could be acquired with a total data rate of 115200 baud. The control of system parameters and the signal processing are performed on a PC using LabVIEW software.

Use of low-power mode of the Wi-Fi transmitter (1 - 2 dBm) provides a longer battery charging interval (about 15 hours in case of using one LDC1000 sensor module and 1.2 Ah battery) and lesser disturbances. The interface cable is also screened for better SNR of measurements.

B. LDC1000 Sensor Module

The sensor module is employing the LDC1000 converter also contains a microcontroller, supply voltage regulator, RS - 485 interface driver and a switched capacitor voltage converter that produces 5V supply for the output stage of the LDC1000 converter, Fig. 3. In the current experiments, the sampling rate of the sensor module was set to 60 Hz by the master controller.

Both, the equivalent parallel resonance impedance R_p, and resonant frequency of an LC resonator f_R are measured simultaneously. However, since the physiological activity reflects in the f_R significantly less than in R_p the resonant frequency is used only for the characterization of the properties of the sensor resonator. Maximum f_R is limited to 5 MHz by the properties of LDC1000.

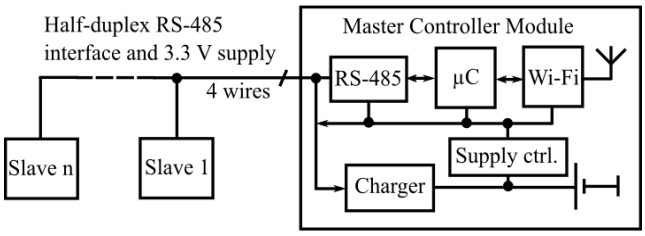

Fig. 2. Overview of the measurement system.

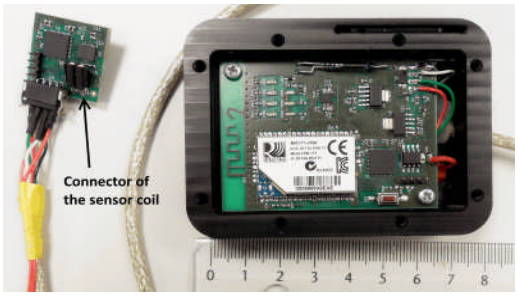

Fig. 3. A photo of the LDC1000 sensor module (left) and master controller module (right).

IV. Sensor Coils and the Imitator of Lungs

A. Sensor Coils

The sensitivity of detection of the physiological activity of lungs depends on several parameters of the measurement setup including:

1) Diameter d and a shape of the sensor coil;
2) Number of windings of the coil n;
3) A distance from the body l;
4) Resonant frequency of the LC resonator f_R;
5) Initial impedance R_p of the LC resonator.

To ensure the stability of coil dimensions they were wound using the plastic form, Fig. 4. These forms were also used for the well-determined positioning of sensor coils at the back of thorax of volunteers and near the imitator of lungs. The sensor and master controller modules are placed on the back side of the form. The plastic form itself is fixed using an elastic belt.

The main properties of sensor coils are given in Table I. The initial parameters of coils, L_p and R_{p1} are measured with the Wayne Kerr Precision Impedance Analyzer 6500B using fixed capacitor C_p = 330 pF. R_{p2} is measured with the LDC1000 sensor module. In this case, the stray capacitance of the sensor increases the value of C_p by 27 pF. Also, the initial value of R_{p2} is less than R_{p1} since it is affected by the output impedance of the sensor circuitry.

All the coils are made of isolated stranded wire with the outside diameter 2 mm and cross-section area 0.75 mm^2. The planar wraparound is used for the lesser height of the sensor that is required in practical implementations. The diameter d is measured between the centers of the coil shape.

The coils 2, 4, 5, and 6 are equipped with a flexible ferrite sheet (type IRL02, TDK Corporation) that is placed in between the plastic form and a coil. This polymeric ferrite sheet with a permeability 25, thickness 1 mm, and low losses at frequencies up to 15 MHz, concentrates the magnetic flux toward a thorax and screens the back side of the coil. Use of the ferrite also allows the placement of the sensor module near the coil without additional screening.

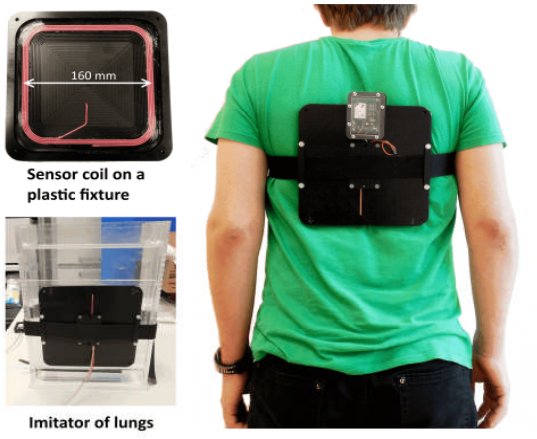

Fig. 4. Photos of the sensor coil on a plastic form, it's placement on the imitator of lungs, and at the back of thorax of a volunteer.

TABLE I. Specification of Sensor Coils with C_p 330 pF

Coil No.	d, mm	n	L_{coil}, µH	f_R, MHz	R_{p1}, kΩ	R_{p2}, kΩ	Note
1	161	4	7.41	3.16	19.0	14.0	
2	161	4	9.70	2.76	17.9	14.2	a
3	155	8	22.60	1.81	39.4	n/a	
4	155	8	28.75	1.59	34.9	28.2	a
5	146	12	53.57	1.18	44.9	40.5	a
6	75	8	11.76	2.51	20.0	14.7	a

[a.] the back side of the coil is shielded with a flexible ferrite sheet

B. Imitator of the Impedance of Lungs, IIL

The physiological activity modulates the reflected impedance in several ways as described in the section II*B*. It is complicated to ensure the repeatability of these activities. Furthermore, the influence of the physiological activity of persons varies significantly. To improve the reliability of comparison of the parameters of different sensors, the imitator of the impedance of lungs (IIL) was designed.

IIL is a reservoir made of Plexiglas with the inner dimensions 238 × 115 × 350 mm (Fig. 4). In the both sides of the reservoir are guides for the insertion of the perforated partition walls also made of 10 mm Plexiglas.

The reservoir is filled with a saline solution up to the level of 300 mm (without a partition wall). The conductivity of the solution is chosen equal to the typical expiratory impedance of lungs at 2.6 MHz [4], 0.38 S/m. Sliding the partition wall on and off allows imitation of the change of the of lung's impedance. In the current experiments, one partition wall with a distance of 10 mm from the front side was used. The thickness of the front side of the reservoir is 3 mm, and the minimum distance of the sensor coil from it is 2 mm.

V. Measurement Results

The resonant frequencies and impedances of sensors are given in Table II. The resonant frequencies f_{R2} and impedances R_{p2_1} correspond to the placement of sensors close to IIL without the partition wall. The resonant frequency f_{R2} is kept nearly equal using different values of C_p. The changes of the resonant frequency, df_{R2}, and impedance, dR_{p2}, are recorded in the same position but with the partition wall inserted. The impedance change is calculated against the mean value of the impedance in an observation window.

TABLE II. Impedance and Resonant Frequency of Sensor Coils

Parameter	No. of the sensor coil				
	1	*2*	*4*	*5*	*6*
f_{R2}, MHz	2.73	2.70	2.55	2.56	2.48
df_{R2}, %	0.00	0.13	0.12	0.00	0.00
R_{p2_1}, kΩ	10.93	11.92	22.45	32.33	13.47
d R_{p2}, %	-3.48	-3.19	-2.00	-1.73	-1.41

A change of the impedance caused by the volume of the partition wall characterizes the sensitivity of sensors. This 0.87-liter volume change corresponds to 10.63 % change of the initial volume of the saline solution in IIL.

From the data given in Table II, it follows that the sensitivity of the sensor increases with the diameter of the sensor coil (coils No. 6 and 4). It also follows that the sensor with 4 windings (coils No 1 and 2) have higher sensitivity than sensors with 8 and 12 windings (coils No 4 and 5).

The use of the flexible ferrite sheet has a low impact on the sensitivity of the sensors (coils No 1 and 2). However, it screens the back side of the coil, which allows the placement of the sensor and master controller modules near the coil.

Dependence of the sensitivity of coils No. 2 and 4 on a resonant frequency f_{R2} is illustrated in Fig. 5. Unfortunately, the frequency range above 5 MHz is not tested due to the limitation of the LDC1000 converter.

Fig. 6 illustrates a dependence of the impedance of the sensor coil No. 2 on a distance from the IIL. R_{p2_1} corresponds to the impedance without the partition wall and R_{p2_2} to the impedance with partition wall inserted. The sensitivity of the sensor is characterized by dR_{p2}. The lower curve of normalized sensitivity dR_{p2_d} shows the change of R_{p2_1} that is caused by 1 mm change of the distance of the sensor coil from the IIL.

The waveforms of the respiration signal and an accompanying artifact is shown in Fig. 7. These additional signals can be used for the classification of human motion [5]. However, for the respiration monitoring, the artifacts must be suppressed since the output signal of the sensor is a sum of all components.

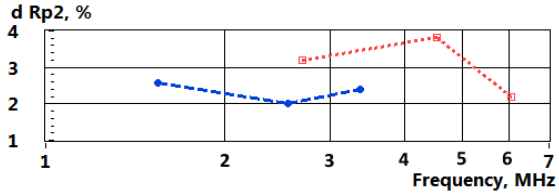

Fig. 5. Dependence of the sensitivity of coils No. 2 (upper curve).and 4 (lower curve) on a resonant frequency f_{R2}.

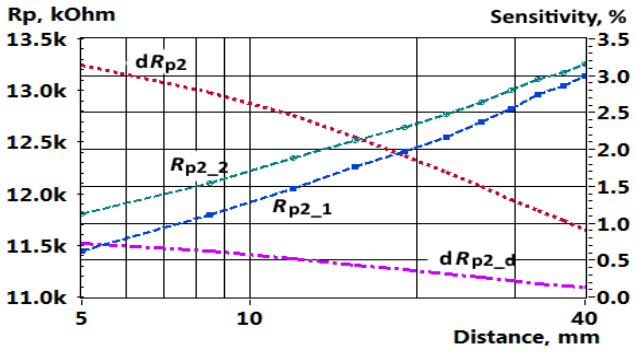

Fig. 6. Influence of the distance of the coil No. 2 from the IIL on the impedances R_{p2_1}, R_{p2_2}, sensitivity dR_{p2}, and normalized sensitivity dR_{p2_d}.

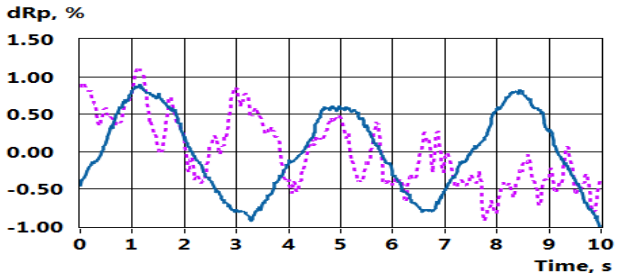

Fig. 7. The waveform of a respiration signal (solid line) and a signal induced by walking (dashed line) in case of bated breathing.

If the ferrite sheet is not used, an inductive coupling between the coil and elements of sensor module could significantly change the measurement results. As an example, the initial impedance of the sensor coil No. 3, R_{p2}, was unstable and has higher values than R_{p1}, which is unrealistic.

VI. Conclusions

The design of the respiration telemonitoring system using a single coil magnetic induction sensor and high-resolution LDC1000 converter is described.

The parameters of the system are tested with different sensor coils and the imitator of the impedance of lungs. Measurements in healthy volunteers demonstrated the ability of the system to monitor respiration.

However, the tests show a significant influence of the motion artifacts on the measured respiration signals. The changes of the distance of the sensor coil from the body also have considerable impact. Suppression and compensation of these influences is a topic of further research.

Acknowledgment

This research was supported by the European Union through the European Regional Development Fund in frames of the research center CEBE and competence center ELIKO, partly also by Estonian Research Council (IUT19-11-2014).

References

[1] P. Tarjan, R. McFee, “Electrodeless measurements of the effective resistivity of the human torso and head by magnetic induction,” IEEE Trans. Biomed. Eng. vol. 15, pp. 266-278, 1968.

[2] L. Humal, J. Vedru, “Physiological measurement based on Foucault principle: Set-up of the problem,” Med. Biol. Eng. Comput. vol. 15, pp. 183–184, 1996.

[3] D. Teichmann, A. Kuhn, S. Leonhardt, M. Walter, “The MAIN Shirt: A Textile-Integrated Magnetic Induction Sensor Array,” Sensors, vol. 14(1), pp. 1039-1056, 2014.

[4] D. Andreuccetti, R. Fossi, C. Petrucci: “An Internet resource for the calculation of the dielectric properties of body tissues in the frequency range 10 Hz - 100 GHz,” http://niremf.ifac.cnr.it/tissprop/. IFAC-CNR, Florence (Italy), 1997. Based on data published by C.Gabriel et al. in 1996.

[5] D. Teichmann, A. Kuhn, S. Leonhardt, M. Walter, “Human motion classification based on a textile integrated and wearable sensor array,” Physiol. Meas., vol. 34, pp. 963–975, 2013.